

# Doppler Myocardial Imaging to Evaluate the Effectiveness of Pacing Sites in Patients Receiving Biventricular Pacing

Gerardo Ansalone, MD,\* Paride Giannantoni, MD,\* Renato Ricci, MD,\* Paolo Trambaiolo, MD,† Francesco Fedele, MD,‡ Massimo Santini, MD, FACC, FESC

Rome, Italy

---

<b>OBJECTIVES</b>	The goal of this study was to compare the efficacy of biventricular pacing (BIV) at the most delayed wall of the left ventricle (LV) and at other LV walls.
<b>BACKGROUND</b>	Biventricular pacing could provide additional benefit when it is applied at the most delayed site.
<b>METHODS</b>	In 31 patients with advanced nonischemic heart failure, the activation delay was defined, in blind before BIV, by regional noninvasive Tissue Doppler Imaging as the time interval between the end of the A-wave (C point) and the beginning of the E-wave (O point) from the basal level of each wall. The left pacing site was considered concordant with the most delayed site when the lead was inserted at the wall with the greatest regional interval between C and O points (CO <sub>R</sub> ). After BIV, patients were divided into group A (13/31) (i.e., paced at the most delayed site) and group B (18/31) (i.e., paced at any other site).
<b>RESULTS</b>	After BIV, in all patients LV end-diastolic (LVEDV) and end-systolic (LVESV) volumes decreased ( $p = 0.025$ and $0.001$ ), LV ejection fraction (LVEF) increased ( $p = 0.002$ ), QRS narrowed ( $p = 0.000$ ), New York Heart Association class decreased ( $p = 0.006$ ), 6-min walked distance (WD) increased ( $p = 0.046$ ), the interval between closure and opening of mitral valve (CO) and isovolumic contraction time (ICT) decreased ( $p = 0.001$ and $0.000$ ), diastolic time (EA) and Q-P <sub>2</sub> interval increased ( $p = 0.003$ and $0.000$ ), while Q-A <sub>2</sub> interval and mean performance index (MPI) did not change. Group A showed greater improvement over group B in LVESV ( $p = 0.04$ ), LVEF ( $p = 0.04$ ), bicycle stress testing work ( $p = 0.03$ ) and time ( $p = 0.08$ ) capacity, CO ( $p = 0.04$ ) and ICT ( $p = 0.02$ ).
<b>CONCLUSIONS</b>	After BIV, LV performance improved significantly in all patients; however, the greatest improvement was found in patients paced at the most delayed site. (J Am Coll Cardiol 2002;39:489-99) © 2002 by the American College of Cardiology

---

In patients receiving biventricular pacing (BIV), the site of the left ventricle (LV) lead varies randomly for several anatomical and technical reasons so that LV pacing cannot be applied at the most delayed wall in all patients. Since the rationale of BIV is to stimulate the most delayed LV wall (1-5), the left pacing site could provide additional benefit when it is concordant with the most delayed site. Our observational study aimed to define the most delayed wall by tissue Doppler imaging (TDI) (6-9) and to verify whether LV performance showed a greater improvement in patients paced at the most delayed site compared with patients paced at any other site.

## METHODS

**Inclusion criteria.** We studied 31 patients with nonischemic heart failure (HF) and left bundle branch block (LBBB) who were referred to our institution from January 1999 to January 2001. The inclusion criteria were: patients with severe HF, still symptomatic (New York Heart Asso-

ciation [NYHA] class III or IV) after optimal drug treatment involving diuretics, converting enzyme inhibitors at the maximum tolerated dose and beta-adrenergic blocking agents with: LV systolic dysfunction defined by ejection fraction <40%, permanent LBBB, normal sinus rhythm, at least one hospitalization for HF in the year before inclusion, drug-induced stability for at least three months before inclusion and successful BIV implantation. All patients underwent coronary angiography. For reference, 18 of these 31 patients were included in an earlier study to analyze qualitative patterns of LV activation.

**Standard echocardiography.** All the studies were performed with a commercially available ultrasonographic system (Acuson, Sequoia, Mountain View, California). The echocardiographic study was performed in baseline condition, the day before and the day after pacemaker implantation, that is, respectively, in sinus rhythm (SR) and BIV. Detailed two-dimensional and M-mode echocardiography was obtained under American Society of Echocardiography guidelines to measure the following parameters: 1) LV end-diastolic volume (LVEDV); 2) LVEDV index (LVEDVI) (i.e., LVEDV/body surface area); 3) LV end-systolic volume (LVESV); 4) LVESV index (LVESVI) (i.e., LVESV/body surface area); 5) LV ejection fraction

From the \*Department of Heart Diseases, San Filippo Neri Hospital, Rome, Italy; †Department of Cardiology, Sandro Pertini Hospital, Rome, Italy; and the ‡Department of Cardiac and Respiratory Sciences of University "La Sapienza," Rome, Italy.

Manuscript received April 4, 2001; revised manuscript received October 10, 2001, accepted October 31, 2001.

**Abbreviations and Acronyms**

BIV	= biventricular pacing
CO	= time between closure and re-opening of mitral valve
CO <sub>R</sub>	= time between the end of regional A-PW and the beginning of E-PW
EA	= left ventricular diastolic time
HF	= heart failure
ICT	= left ventricular isovolumetric contraction time
IRT	= left ventricular isovolumetric relaxation time
IVS	= interventricular septum
LBBB	= left bundle branch block
LV	= left ventricle
LVEDV	= left ventricular end-diastolic volume
LVEDVI	= left ventricular end-diastolic volume index
LVEF	= left ventricular ejection fraction
LVESV	= left ventricular end-systolic volume
LVESVI	= left ventricular end-systolic volume index
LVET	= left ventricular ejection time
M-mode	= M-mode color Doppler
MPI	= left ventricular mean performance index
MUGA	= multigated equilibrium blood pool scintigraphy
NYHA	= New York Heart Association
PW	= pulsed-wave
Q-A <sub>2</sub>	= left ventricular electromechanical systole
Q-P <sub>2</sub>	= right ventricular electromechanical systole
RV	= right ventricle
SR	= sinus rhythm
TDI	= tissue Doppler imaging
WD	= 6-min walked distance

(LVEF) assessed using the modified biplane Simpson rule (10). The LV volumes and LVEF were calculated as the average of three different blind measurements by two echocardiographers. The standard echo-Doppler approach was applied to measure transmitral, aortic and pulmonary flow velocities with a 2.5 MHz to 5.0 MHz pulsed-wave (PW) Doppler in the four-chamber apical and parasternal views. The following systolic and diastolic time intervals were measured before and after BIV: 1) LV electromechanical systole (Q-A<sub>2</sub>); 2) RV electromechanical systole (Q-P<sub>2</sub>); 3) LV pre-ejection period; 4) RV pre-ejection period; 5) LV electromechanical interval from Q-wave to mitral closure; 6) LV isovolumic contraction time (ICT) from mitral closure to beginning of the aortic flow; 7) RV ejection time; 8) LV ejection time (LVET); 9) isovolumic LV relaxation time (IRT) from A<sub>2</sub> closure to mitral opening; 10) time between closure and re-opening of mitral valve (CO); 11) diastolic time (EA); 12) mean performance index (MPI) measured by the difference between CO and LVET normalized for LVET [(CO - LVET)/LVET]. All intervals were expressed in corrected units (c.u. = measured interval/√R-R interval).

**Tissue Doppler Imaging (TDI).** Tissue Doppler imaging was performed in M-mode color Doppler (M-mode) and PW Doppler modalities from the apical view to assess longitudinal myocardial regional function analyzing, respectively, interventricular septum (IVS), inferior, posterior,

lateral and anterior walls. In PW, the velocity profiles were recorded with a sample volume placed in the middle of the basal segment of each wall. Gain and filters were adjusted as needed to eliminate background noise and allow for a clear tissue signal. Tissue Doppler imaging velocities (from -30 to 30 cm/s) were recorded at a sweep speed of 100 mm/s and stored digitally on a magneto-optical disk. In M-mode, the scanned sector was acquired with two-dimensional and M-mode gray scale imaging set at zero level, with the color-coded scale set at the highest level.

**Regional time intervals.** The following systolic and diastolic time intervals were detected regionally at each wall using PW and M-mode modalities: 1) CO interval (CO<sub>R</sub>), lengthening from the end of the A-PW to the beginning of the E-PW or from the end of the last blue component of the preceding cycle to the beginning of the first homogeneous blue diastolic M-mode component; 2) EA interval (EA<sub>R</sub>), detected from the beginning of the E-PW to the end of the A-PW, or from the end of the third red systolic M-mode component to the end of the blue diastolic M-mode component; 3) isovolumic contraction time (ICT<sub>R</sub>) lengthening from the beginning of the S<sub>1</sub>-PW to the beginning of the S<sub>2</sub>-PW, or from the beginning of the first red systolic M-mode component to the beginning of the second red systolic M-mode component; 4) isovolumic relaxation time (IRT<sub>R</sub>) lengthening from the end of the S<sub>2</sub>-PW to the beginning of the E-PW or from the end of the second red systolic M-mode component to the end of the third red systolic M-mode component; 5) LVET<sub>R</sub> resulting from the difference between the CO<sub>R</sub> and the sum of ICT<sub>R</sub> + IRT<sub>R</sub> [i.e., CO<sub>R</sub> - (ICT<sub>R</sub> + IRT<sub>R</sub>)]; 6) mean performance index (MPI<sub>R</sub>) estimated using the rule (CO<sub>R</sub> - LVET<sub>R</sub>)/LVET<sub>R</sub>. All intervals were measured in PW modality and expressed in c.u.

**Assessment of regional delay.** The CO<sub>R</sub> was selected to assess the regional mechanical delay in LV activation; it was calculated at each wall in M-mode and PW modalities, in c.u. for at least three beats. The most delayed site was identified from the maximum CO<sub>R</sub> in each patient before BIV, in blind to avoid any bias in the choice of pacing site.

**Concordance between the delayed site and the pacing site.** We identified the pacing site by analyzing the frontal, lateral, right and left oblique X-ray views. The lead position was classified as lateral, posterior, inferior or anterior according to the anatomy of the branches of the coronary sinus (11). Then, a correlation between the site of pacing (X-ray defined) and the site of delay (TDI defined) was assessed in blind by two observers with 100% concordance. On the basis of such a correlation, when the catheter was placed at the wall where the CO<sub>R</sub> achieved maximum value, the pacing site was considered coincident with the most delayed wall. The only exception was the IVS because left pacing is not feasible at this site for anatomic reasons. Thus, when the maximum CO<sub>R</sub> was detected at the IVS and the inferior wall paced, the latter was considered concordant with the site of the delay, provided that it showed the longest CO<sub>R</sub> after that of the IVS. On the basis of the

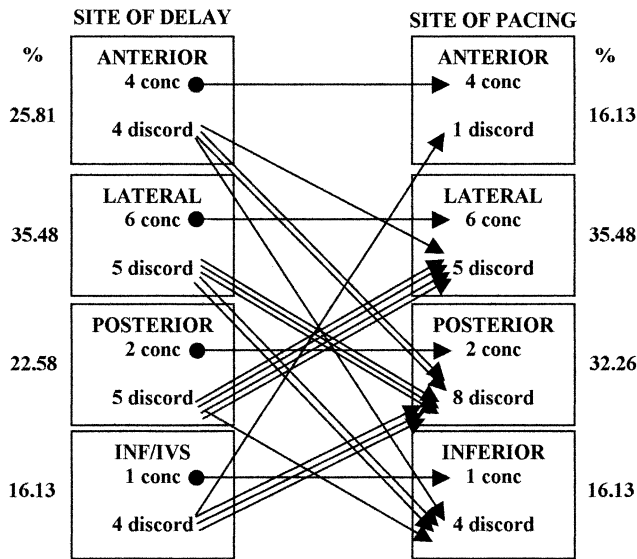


**Figure 1.** Diagram showing the correlation between the most delayed site and pacing site in 31 biventricular pacing (BIV) patients.

concordance or discordance between the pacing site and the delayed site, patients were divided into group A: patients paced at the site of the greatest delay, and group B: patients paced at any other site. Two-dimensional and TDI parameters, NYHA class, exercise tolerance and QRS narrowing were compared in the two groups before and after BIV.

**Exercise tolerance.** All patients underwent maximal and/or symptom-limited bicycle stress testing using an incremental protocol of 10 W/min until the maximum tolerated workload was reached. The test was performed the day before implantation during spontaneous SR and one week later during BIV. The 6-min walking test was also performed before and after BIV.

**Clinical evaluation.** A skilled HF physician evaluated NYHA class before (<1 week) and after (>1 week <1 month) implantation.

**Statistical analysis.** Data are presented as mean  $\pm$  SD for continuous variables. The differences in all patients and in each subgroup were validated using a two-way repeated measures analysis of variance.

## RESULTS

**Regional delay compared with the pacing site.** The  $CO_R$  ranged from  $19.10 \pm 1.36$  c.u. at the IVS to  $20.22 \pm 1.86$  c.u. at the lateral wall, with a  $\Delta-CO_R = 1.12$ . The IVS was the most delayed wall ( $CO_R = 21.07$  c.u.) in only one patient, who was paced at the inferior wall, which was, in turn, substantially delayed ( $CO_R = 21.05$  c.u.). Therefore, this patient was included in group A. Figure 1 shows the prevalence of the most delayed sites together with the random distribution of blind chosen pacing sites. Before BIV, the lateral wall was the most frequently delayed (35.5%), followed by anterior (25.8%), posterior (22.6%)

**Table 1.** Echocardiographic, Exercise and Clinical Variables in All, Group A and Group B

Variables		Group			ANOVA (p)	
		All	A	B	Spont/BIV	A/B
LVEDV	Spont	173.4 $\pm$ 76.8	197.2 $\pm$ 97.7	156.2 $\pm$ 54.1	0.025	0.51
	BIV	157.1 $\pm$ 73.5	175.5 $\pm$ 89.6	143.8 $\pm$ 58.4		
LVEDVi	Spont	96.2 $\pm$ 41.8	107.6 $\pm$ 55.3	87.9 $\pm$ 27.4	0.026	0.52
	BIV	87.0 $\pm$ 39.7	95.4 $\pm$ 50.4	80.9 $\pm$ 30.0		
LVESV	Spont	120.9 $\pm$ 59.6	140.2 $\pm$ 77.5	106.8 $\pm$ 39.1	0.001	0.04
	BIV	103.6 $\pm$ 58.3	111.8 $\pm$ 69.9	97.6 $\pm$ 49.5		
LVESVi	Spont	67.1 $\pm$ 32.5	76.6 $\pm$ 43.6	60.3 $\pm$ 20.1	0.001	0.05
	BIV	57.4 $\pm$ 31.3	60.7 $\pm$ 38.4	54.9 $\pm$ 25.9		
LVEF	Spont	0.31 $\pm$ 0.07	0.31 $\pm$ 0.08	0.32 $\pm$ 0.05	0.002	0.04
	BIV	0.37 $\pm$ 0.10	0.40 $\pm$ 0.12	0.34 $\pm$ 0.10		
Ex Time	Spont	441.7 $\pm$ 153.5	457.7 $\pm$ 157.1	430.2 $\pm$ 154.4	0.174	0.08
	BIV	460.8 $\pm$ 157.2	506.0 $\pm$ 178.2	428.2 $\pm$ 136.0		
Ex Load	Spont	75.8 $\pm$ 25.7	78.5 $\pm$ 27.8	73.9 $\pm$ 24.8	0.136	0.03
	BIV	79.2 $\pm$ 25.8	87.5 $\pm$ 28.5	73.2 $\pm$ 22.6		
6-min WD	Spont	373 $\pm$ 74	381 $\pm$ 89	368 $\pm$ 64	0.046	0.19
	BIV	391 $\pm$ 80	412 $\pm$ 92	376 $\pm$ 70		
QRS	Spont	160.3 $\pm$ 27.3	170.0 $\pm$ 33.4	153.3 $\pm$ 20.0	0.000	0.72
	BIV	122.6 $\pm$ 24.2	130.0 $\pm$ 23.4	117.2 $\pm$ 24.0		
NYHA	Spont	3.0 $\pm$ 0.2	3.0 $\pm$ 0.0	3.1 $\pm$ 0.2	0.006	0.45
	BIV	2.7 $\pm$ 0.6	2.5 $\pm$ 0.5	2.8 $\pm$ 0.6		

ANOVA = analysis of variance; BIV = biventricular pacing; Ex Load = exercise maximum work load (watts); Ex Time = exercise maximum time (s); LVEDV = left ventricular end-diastolic volume (ml); LVEDVi = LVEDV/body surface area (ml/m<sup>2</sup>); LVEF = left ventricular ejection fraction; LVESV = left ventricular end-systolic volume (ml); LVESVi = LVESV/body surface area (ml/m<sup>2</sup>); NYHA = New York Heart Association; p = statistical significance accepted as p  $\leq$  0.05; Spont = spontaneous rhythm; 6-min WD = 6-min walked distance (meters).

**Table 2.** Global Time Intervals in All, Group A and Group B

Variable		Group			ANOVA (p)	
		All	A	B	Spont/BIV	A/B
CO	Spont	16.72 ± 1.73	16.99 ± 1.81	16.53 ± 1.69	0.001	0.04
	BIV	15.43 ± 2.24	14.79 ± 2.08	15.89 ± 2.29		
EA	Spont	13.52 ± 2.39	12.91 ± 1.88	13.97 ± 2.67	0.003	0.25
	BIV	14.81 ± 2.35	14.75 ± 2.39	14.85 ± 2.38		
QA <sub>2</sub>	Spont	13.80 ± 1.29	14.38 ± 0.98	13.38 ± 1.35	0.130	0.08
	BIV	14.15 ± 0.95	14.26 ± 1.09	14.07 ± 0.86		
QP <sub>2</sub>	Spont	12.77 ± 0.98	12.86 ± 0.67	12.71 ± 1.18	0.000	0.70
	BIV	14.10 ± 1.03	14.04 ± 1.19	14.15 ± 0.92		
ICT	Spont	3.67 ± 1.14	4.12 ± 1.17	3.34 ± 1.02	0.000	0.02
	BIV	2.19 ± 1.05	2.17 ± 1.09	2.20 ± 1.06		
IRT	Spont	3.52 ± 1.19	3.42 ± 0.86	3.60 ± 1.40	0.519	0.74
	BIV	3.33 ± 1.35	3.34 ± 1.30	3.32 ± 1.42		
MPI	Spont	0.77 ± 0.26	0.75 ± 0.28	0.78 ± 0.25	0.109	0.22
	BIV	0.68 ± 0.36	0.59 ± 0.36	0.75 ± 0.35		

All intervals were measured in corrected units (c.u. = measured interval/ $\sqrt{N}$  preceding RR).

ANOVA = analysis of variance; BIV = biventricular pacing; CO = interval between the mitral valve closing and re-opening; EA = diastolic lengthening of the LV; ICT = isovolumic contraction time; IRT = isovolumic relaxation time; MPI = mean performance index; QA<sub>2</sub> = interval between Q-wave and aortic valve closing; QP<sub>2</sub> = interval between Q-wave and pulmonary valve closing; Spont = spontaneous rhythm.

and IVS and/or inferior walls (16.13%). A total of 13/31 patients (41.9%) were paced at the most delayed site, while 18/31 patients (58.1%) were paced at a discordant site. The most widely paced site was the lateral wall (35.5%), followed by posterior (32.3%) and anterior (16.1%) or inferior wall (16.1%).

**QRS duration.** QRS narrowed significantly in all ( $p = 0.000$ ), with no significant decrease in groups A or B (Table 1).  
**Echocardiographic data.** After BIV, in all LVEDV, LVEDVi, LVESV and LVESVi decreased significantly ( $p = 0.025, 0.026, 0.001$  and  $0.001$ , respectively), while LVEF increased significantly ( $p = 0.002$ ) (Table 1). How-

**Table 3.** Regional Time Intervals in All, Group A, and Group B

Variable		Group			ANOVA (p)	
		All	A	B	Spont/BIV	A/B
CO Ivs	Spont	19.22 ± 1.36	19.85 ± 1.05	18.77 ± 1.39	0.000	0.03
	BIV	17.42 ± 1.11	17.40 ± 1.06	17.43 ± 1.17		
CO Inf	Spont	19.61 ± 1.19	19.90 ± 0.81	19.40 ± 1.39	0.000	0.33
	BIV	18.03 ± 1.01	18.08 ± 0.98	17.99 ± 1.06		
CO Lat	Spont	19.91 ± 1.86	20.58 ± 1.29	19.43 ± 2.09	0.000	0.31
	BIV	18.11 ± 1.73	18.52 ± 1.48	17.82 ± 1.88		
CO Pos	Spont	19.86 ± 1.78	20.36 ± 1.30	19.45 ± 2.04	0.000	0.35
	BIV	17.96 ± 1.69	18.01 ± 1.59	17.92 ± 1.80		
CO Ant	Spont	19.71 ± 1.63	20.22 ± 1.08	19.35 ± 1.88	0.000	0.30
	BIV	17.86 ± 1.70	18.01 ± 1.69	17.76 ± 1.75		
EA Ivs	Spont	11.05 ± 2.48	9.77 ± 1.88	11.98 ± 2.48	0.001	0.04
	BIV	12.45 ± 2.01	12.09 ± 2.06	12.71 ± 1.99		
EA Inf	Spont	10.73 ± 2.74	9.97 ± 2.32	11.29 ± 2.94	0.003	0.37
	BIV	11.96 ± 2.11	11.60 ± 2.27	12.23 ± 2.00		
EA Lat	Spont	10.40 ± 2.93	9.04 ± 1.51	11.38 ± 3.33	0.001	0.08
	BIV	11.91 ± 2.64	11.38 ± 2.19	12.30 ± 2.92		
EA Pos	Spont	10.46 ± 3.07	9.39 ± 1.91	11.33 ± 3.58	0.004	0.25
	BIV	12.13 ± 2.76	11.79 ± 2.71	12.38 ± 2.84		
EA Ant	Spont	10.61 ± 2.85	9.40 ± 1.33	11.48 ± 3.34	0.003	0.21
	BIV	12.22 ± 2.43	11.75 ± 1.93	12.55 ± 2.75		
IRT Lat	Spont	6.13 ± 1.68	6.32 ± 1.11	5.99 ± 2.01	0.210	0.05
	BIV	5.71 ± 1.58	5.17 ± 1.30	6.11 ± 1.68		
MPI Lat	Spont	1.27 ± 0.49	1.24 ± 0.42	1.30 ± 0.55	0.087	0.02
	BIV	1.46 ± 0.63	1.11 ± 0.36	1.72 ± 0.66		

All intervals were measured in corrected units (c.u. = measured interval/ $\sqrt{N}$  preceding RR).

ANOVA = analysis of variance; BIV = biventricular pacing; CO<sub>ANT</sub> = CO<sub>R</sub> at anterior wall; CO<sub>INF</sub> = CO<sub>R</sub> at inferior wall; CO<sub>IVS</sub> = CO<sub>R</sub> at interventricular septum; CO<sub>LAT</sub> = CO<sub>R</sub> at lateral wall; CO<sub>POS</sub> = CO<sub>R</sub> at posterior wall; EA<sub>ANT</sub> = EA<sub>R</sub> at anterior wall; EA<sub>INF</sub> = EA<sub>R</sub> at inferior wall; EA<sub>IVS</sub> = EA<sub>R</sub> at interventricular septum; EA<sub>LAT</sub> = EA<sub>R</sub> at lateral wall; EA<sub>POS</sub> = EA<sub>R</sub> at posterior wall; IRT<sub>LAT</sub> = isovolumic relaxation time at lateral wall; MPI<sub>LAT</sub> = mean performance index at lateral wall; Spont = spontaneous rhythm.

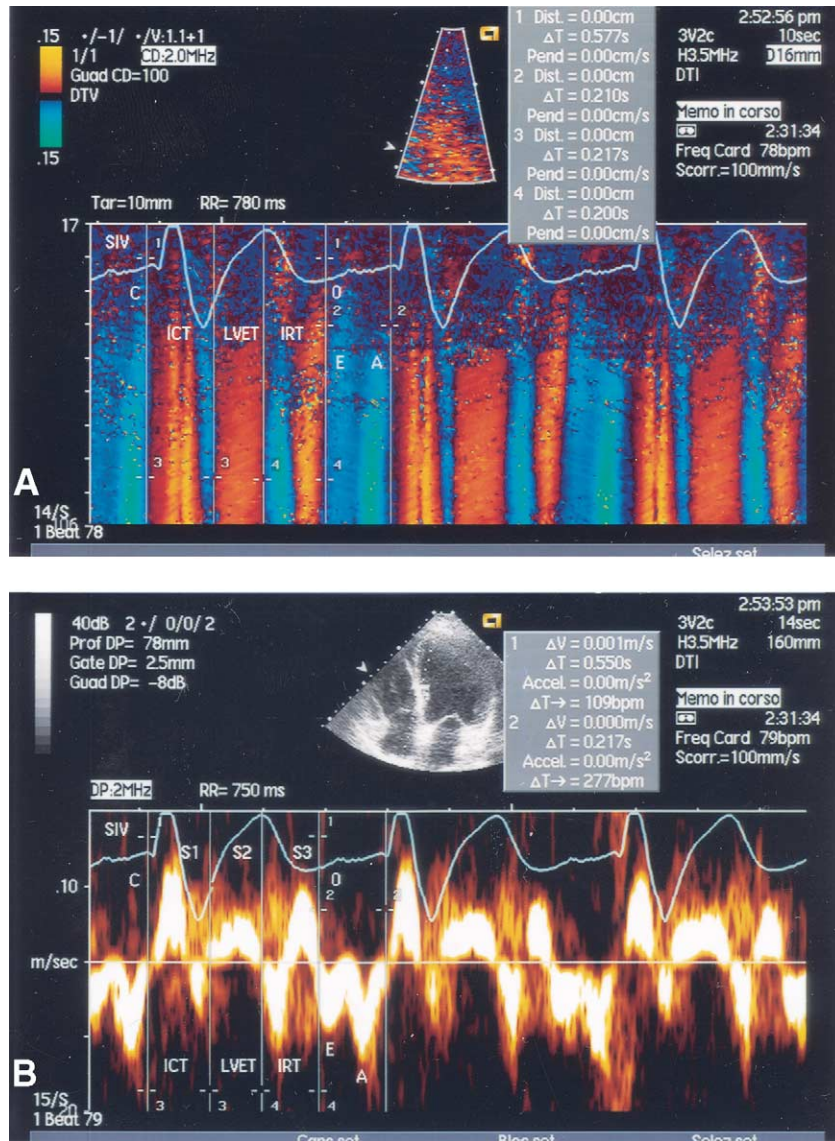


**Figure 2.** (A) M-mode tissue Doppler imaging of the interventricular septum (IVS). When the QRS is prolonged, regional left ventricular isovolumic contraction time ( $ICT_R$ ) is prolonged and split, regional left ventricular ejection time ( $LVET_R$ ) shortens and regional isovolumic relaxation time ( $IRT_R$ ) lengthens considerably, the latter showing a blue-red sequence. Despite an unsynchronized activation of the wall, the movement is still coordinated. Time between closure and re-opening of mitral valve interval ( $CO_R$ ) = 577 ms. (20.6 c.u.); regional EA interval ( $EA_R$ ) = 210 ms;  $ICT_R$  = 217 ms;  $IRT_R$  = 200 ms; preceding RR: 780 ms. Recording velocity 100/mm/s. SIV = interventricular septum (IVS). (B) Pulsed wave-tissue Doppler imaging of the IVS. The strip shows the same pattern of severe unsynchronized activation as in A.  $CO_R$  is longer than  $EA_R$ .  $CO_R$  = 550 ms. (20.14 c.u.);  $EA_R$  = 217 ms; preceding RR: 750 ms.

ever, group A showed greater improvement over group B in LVESV ( $p = 0.04$ ), LVESVi ( $p = 0.05$ ) and LVEF ( $p = 0.04$ ), while LVEDV and LVEDVi showed no significant difference between the two groups (Table 1).

**Exercise tolerance.** After BIV, in all, NYHA class decreased ( $p = 0.006$ ), 6-min walked distance (WD) increased ( $p = 0.046$ ), while bicycle stress testing work and time capacity showed no significant changes (Table 1). Conversely, group A showed greater improvement over group B in exercise work ( $p = 0.03$ ) and time ( $p = 0.08$ ) capacity, while NYHA class and WD showed no further improvement (Table 1).

**Global time intervals.** After BIV, in all, CO and ICT decreased ( $p = 0.001$  and  $0.000$ ), EA and  $Q-P_2$  increased ( $p = 0.003$  and  $0.000$ ), while no significant change was observed in IRT, MPI or  $Q-A_2$  (Table 2). However, group A showed greater improvement over group B in CO ( $p = 0.04$ ) and ICT ( $p = 0.02$ ) decrease (Table 2).

**Regional time intervals.** After BIV, in all,  $CO_R$  and  $EA_R$  improved at every wall ( $p = 0.000$  and at least  $0.004$ ), but improvement was greater in group A at the IVS ( $p = 0.03$  and  $0.04$ ) (Table 3). At the lateral wall,  $IRT_R$  and  $MPI_R$  decreased in group A, while they increased in group B ( $p = 0.05$  and  $0.02$ ) (Table 3).

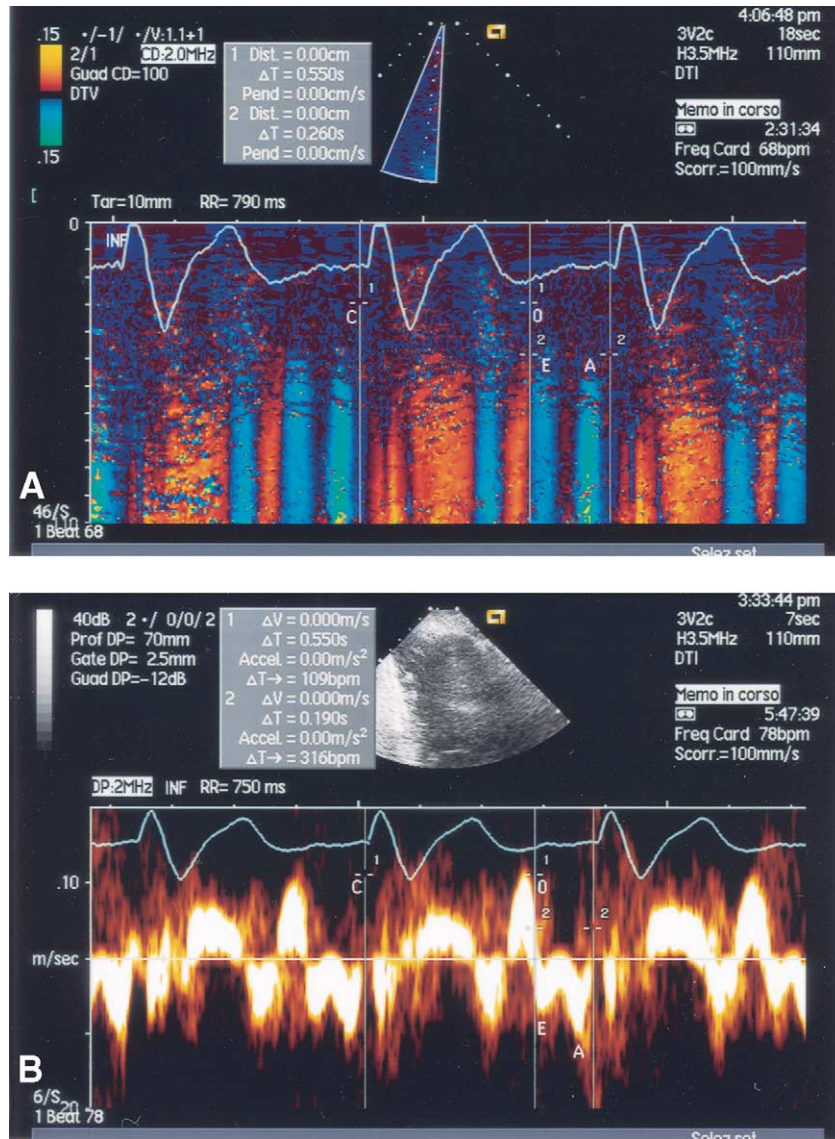


**Figure 3.** (A) M-mode tissue Doppler imaging of the inferior wall. Tissue Doppler imaging pattern is similar to that shown in Figure 2 but with a lesser degree of regional asynchrony. As in Figure 2, CO interval ( $CO_R$ ) is longer than  $EA_R$  but with a gradient of lesser degree ( $CO_R$ : 550 ms >  $EA_R$ : 190 ms in this figure versus  $CO_R$ : 577 ms >  $EA_R$ : 217 ms in the previous figure). Preceding RR: 790 ms;  $CO_R$  = 550 ms (19.5 c.u.);  $EA_R$  = 260 ms. (B) PW-TDI of the inferior wall, showing a mild degree of unsynchronized activation.  $CO_R$  = 550 ms (20.08 c.u.);  $EA_R$  = 190 ms; preceding RR: 750 ms. See Figure 2 for abbreviations.

**Regional myocardial velocities.** After BIV, there were no significant changes in myocardial velocity values in all, group A or group B.

## DISCUSSION

In our previous series, we assessed the regional qualitative TDI patterns due to LBBB and/or HF as well as their changes after BIV (12). These patterns were graduated in a scale reflecting the progression from asynchronous (i.e., delayed) to dyskinetic wall motion of the LV. Such a scale enabled us to compare LV asynchrony before BIV with LV resynchronization after BIV. However, the highest degree

of dyskinetic wall motion does not always correspond to the highest degree of regional delay per se. Since TDI in this field may identify the most delayed site to guide BIV implantation, in this study, first we defined the most delayed site in blind with implantation; second, we evaluated the degree of concordance of the pacing sites (randomly assigned) with the most delayed sites (TDI pre-defined); third, we compared LV performance in patients paced at a concordant site with that in patients paced at a discordant site. Because there was no substantial data on the clinical relevance of such a discordance and TDI had not yet been validated as a reliable method to choose the pacing site, we applied an observational protocol aimed at avoiding any bias

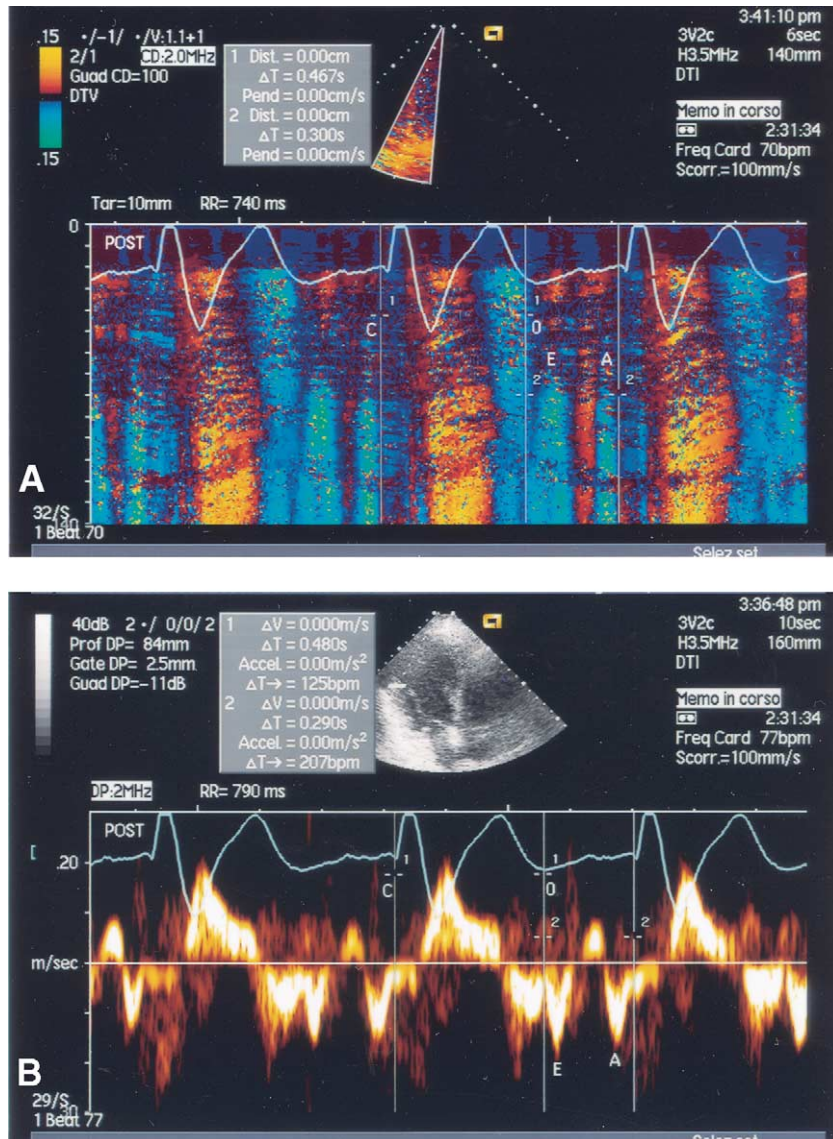


**Figure 4.** (A) M-mode Tissue Doppler imaging (TDI) of the posterior wall showing a dyskinetic motion reversed late in systole. This pattern is characterized by an alternate red and blue systolic sequence, which is due, respectively, to an early movement of the wall toward the transducer (decoded in red) and to a late movement away from the transducer (decoded in blue-green). This pattern is related to a more severe degree of unsynchronized activation, which is responsible for a partially or totally dyskinetic sequence of contraction and relaxation. Such a dyskinetic movement mainly affects the apical level (upper third of TDI panel), while it is quite absent at the basal level (lower third of TDI panel). See the Discussion section for further explanation. CO interval ( $CO_R$ ) = 467 ms (17.16 c.u.);  $EA_R$  = 300 ms; preceding RR: 740 ms. (B) PW-TDI of the posterior wall. In spite of the more severe regional dyskinetic pattern, late reversed in systole,  $CO_R$  and  $EA_R$  are, respectively, shorter and longer than those detected at the inferior wall.  $CO_R$  = 480 ms (17.08 c.u.);  $EA_R$  = 290 ms; preceding RR: 790 ms.

in the selection of pacing site, the latter having already been subjected to several technical and anatomic restrictions due to the complexity of implantation.

**Assessment of regional delay.** To identify the most delayed site we chose the  $CO_R$ , which reflects the delay between two mechanical events (i.e., the beginning of the E-PW and the end of the A-PW); consequently, this interval is strictly related to the regional duration of the mechanical phases of active systole (pre-ejective and ejective contraction) and diastole (post-ejective early relaxation) (13). This parameter is consistent with the time frame

required at each wall to complete the electrical conduction, together with the mechanical activation and active relaxation phases. Thus, the time-frame between the maximum and minimum  $CO_R$ , assessed individually at the basal level of each wall, in itself reflects the regional electromechanical delay in each patient. As shown in Figures 2A to 6A, the  $\Delta-CO_R$  between the IVS and the lateral wall was approximately 100 ms, the  $CO_R$  in M-mode color ranging from a minimum of 450 ms (16.69 c.u.) at the anterior wall and 470 ms (16.61 c.u.) at the lateral wall to a maximum of 577 ms (20.6 c.u.) at the IVS. Furthermore, the M-mode

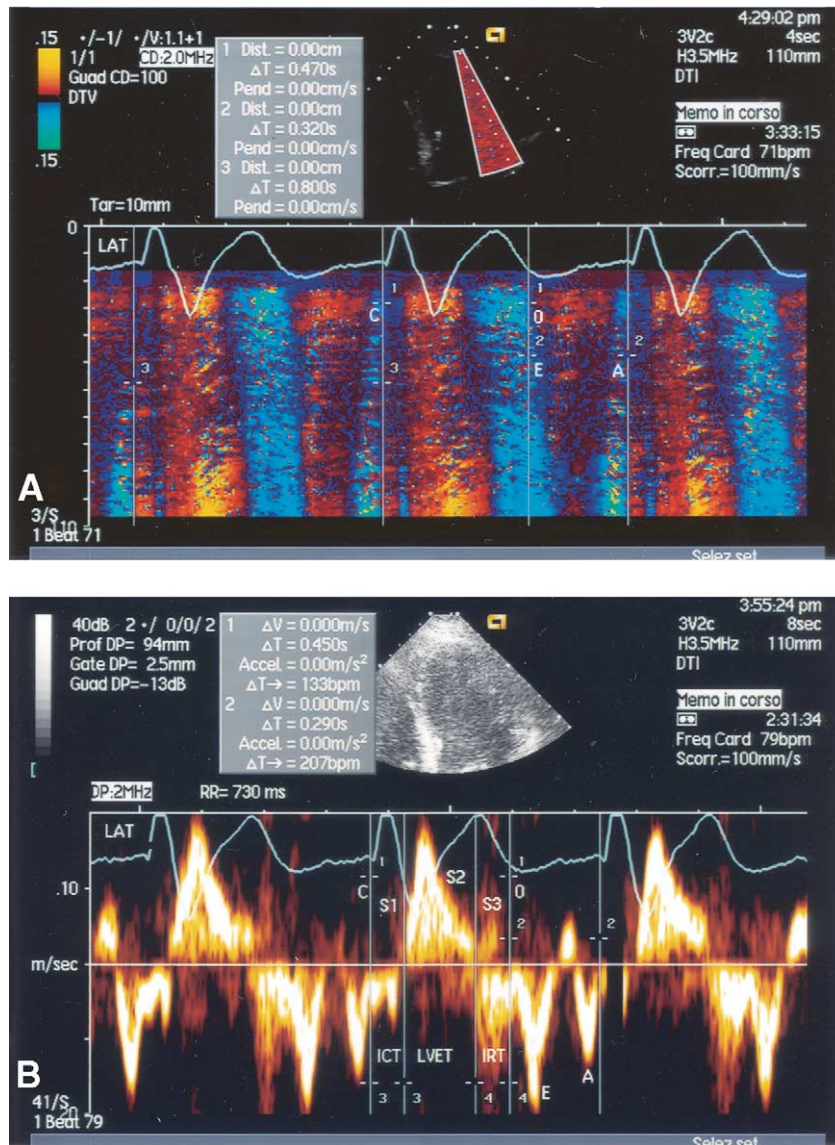


**Figure 5.** (A) M-mode tissue Doppler imaging of the lateral wall, showing a dyskinetic pattern similar to that shown in Figure 4. However, at the lateral wall, CO interval (CO<sub>R</sub>) is shorter, while EA<sub>R</sub> is longer than those observed at the posterior wall. Preceding RR: 800 ms; CO<sub>R</sub> = 470 ms (16.61 c.u.); EA<sub>R</sub> = 320 ms. (B) PW-TDI of the lateral wall, showing the same dyskinetic pattern as in M-mode TDI; CO<sub>R</sub> = 450 ms (16.66 c.u.); EA<sub>R</sub> = 290 ms; ICT<sub>R</sub> = 110 ms; IRT<sub>R</sub> = 110 ms; preceding RR: 730 ms.

TDI pattern at the IVS and inferior wall was characterized by the splitting of the CO<sub>R</sub> into three major red components (i.e., the ICT<sub>R</sub>, the LVET<sub>R</sub> and the IRT<sub>R</sub>), while the direction of the wall movement was always toward the transducer (and, thus, decoded in red). Conversely, the pattern at the lateral and posterior walls was consistent with the splitting of the CO<sub>R</sub> into two main components, indicating a dyskinetic movement directed early toward and late away from the transducer. Such a dyskinetic movement of the lateral wall was related to the shortest CO<sub>R</sub>, whereas the unsynchronized motion of the IVS was associated with the longest CO<sub>R</sub> observed in this patient. The same patterns with more clearly defined signals can be observed in PW modality (Figs. 2B to 6B). By applying this method, we

found that the lateral and posterior were the most frequently delayed walls, together attaining a prevalence of 58.1% of patients, while in the remaining 41.9% of patients the delay was anterior, inferior or at the IVS (Fig. 1). Thus, in spite of the relative prevalence of the delay at the lateral and posterior walls, in more than one-third of cases, a substantial minority of patients, the delay is located at another site from that considered as target wall for left pacing.

**Regional delay compared with the pacing site.** The lack of concordance between the site of delay and the site of pacing is likely to reduce the real benefit in improvement in LV performance due to BIV. In our series, we found 18/31 patients (58.1%) with the delay at the lateral and posterior walls. Even though the lateral and posterior should have



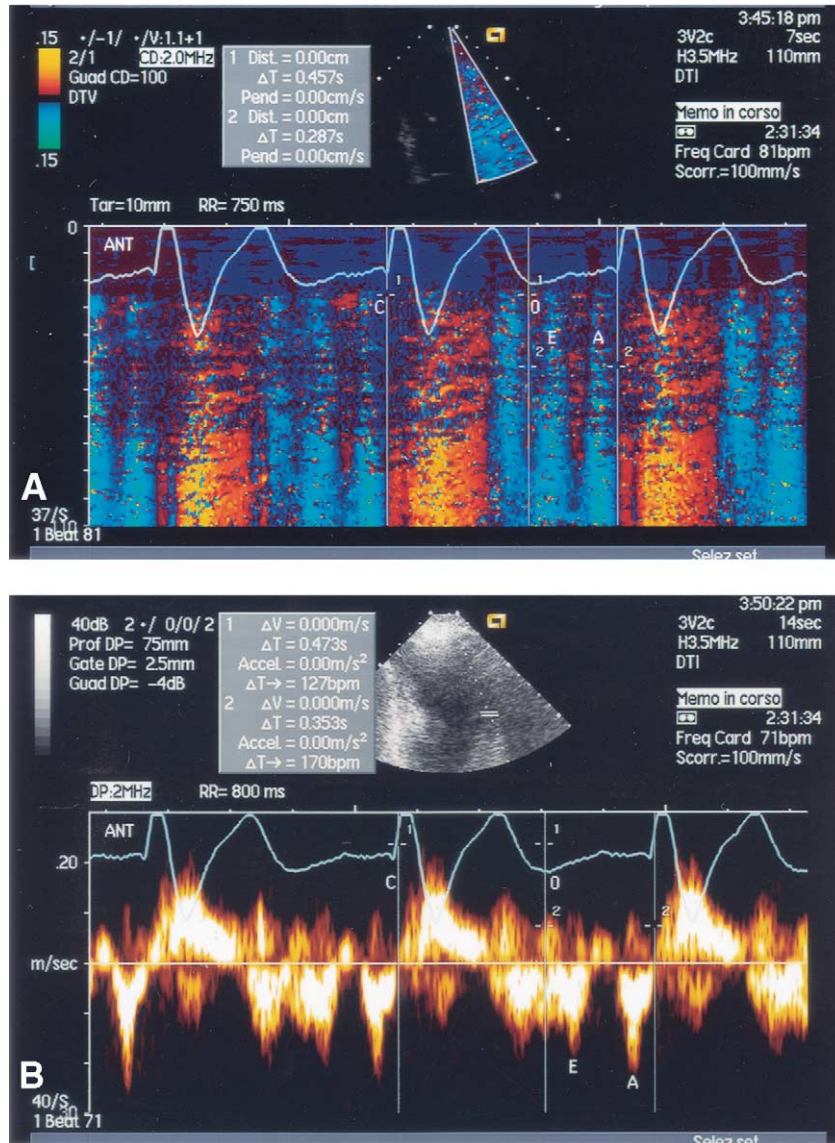


**Figure 6.** (A) M-mode tissue Doppler imaging of the anterior wall. The mechanical activation pattern is quite normal. The CO interval ( $CO_R$ ) lengthens 120 ms less than at the interventricular septum (IVS) ( $457 < 577$  ms), while the  $EA_R$  lengthens approximately 80 ms more than at the IVS ( $287 > 210$  ms). Thus, the gradient observed comparing the  $CO_R$  length at each wall is consistent with the activation delay, which decreases progressively from the IVS to the inferior and posterior walls.  $CO_R = 457$  ms (16.69 c.u.);  $EA_R = 287$  ms; preceding RR: 750 ms. (B) PW-TDI of the anterior wall, showing a quite normal activation pattern.  $CO_R = 473$  ms (16.72 c.u.);  $EA_R = 353$  ms; preceding RR: 800 ms.

been the target walls, in fact, only eight of these (44.4%) were paced at a concordant site. The remaining 10/18 (55.6%) were paced at a discordant site. Thus, the majority of patients who should have been stimulated at the posterior and lateral walls (i.e., the most delayed site) were randomly paced at another site (Fig. 1).

**BIV and LV performance.** Ventricular contraction abnormalities in LBBB patients have been well documented with different noninvasive techniques, such as magnetic resonance (3) or multigated equilibrium blood pool scintigraphy (MUGA) (14), while the improvement in LV performance after BIV has been proven either by hemodynamic study (2,4) or by MUGA measured LVEF or 6-min WD (1).

However, the hemodynamic study is invasive; MRI cannot be applied after BIV, and MUGA should be considered more useful in assessing right and left interventricular dyssynchrony, as recently reported by Saxon et al. (14), than regional intraventricular asynchrony due to LBBB. Thus, to assess the regional intraventricular delay we used TDI, which has been proven useful in detecting quantitatively the regional systolic and diastolic times and velocities within the myocardium (6-9). Conversely, to study LV function, we chose more simple and available methods that may have a wider application, such as two-dimensional systolic parameters and exercise tolerance data. We underline that the diagnostic accuracy of LVEF has been improved by the

enhancement of endocardial border delineation using second harmonic imaging (15), as in our study. After BIV, we observed a significant improvement in all patients, as far as LVEF, NYHA class and 6-min WD are concerned (Table 1). However, as shown by the effects of treatment on all patients compared with the interaction effect of treatment in groups A and B, patients paced at a concordant site derived the greatest benefit from BIV. In fact, in group A we observed a significant decrease in LVEDVi, LVESVi, CO and ICT, which was paralleled by a significant increase in LVEF, EA and bicycle exercise tolerance data (Tables 1 and 2). While bicycle exercise time and load did not improve in all, they improved in group A; conversely, 6-min WD and NYHA class improved in all, with no significant differences in group A. Such a trend toward a clear improvement in exercise time and work load parameters in a small series should be considered more specific than 6-min WD and NYHA class, the latter being easily influenced by the placebo effect. Moreover, in all,  $Q-P_2$  increased significantly, while  $Q-A_2$  did not decrease. Thus, resynchronization therapy may act more by prolonging the electromechanical systole at the RV than by reducing its lengthening at the LV. Interestingly, according to this mechanism,  $Q-A_2$  showed a trend toward a significant increase in group B, while it did not change in group A. Therefore, such a result could also be interpreted in light of the reduction in the interventricular dyssynchrony already documented with MUGA (14). Conversely, after BIV we did not observe any significant difference in IRT nor in MPI (Table 2). This supports the hypotheses that BIV has a beneficial effect on systolic rather than diastolic performance and that such an effect is greater in patients paced at a concordant site. It is noticeable, indeed, that the lengthening of the diastolic filling time (i.e., the EA) increased significantly only in group A. This result should support the hypothesis that BIV is helpful in prolonging (and, thus, improving) the passive diastolic phase when it is applied at a concordant site.

**Regional time intervals.** Where patients were paced at a concordant site,  $IRT_R$  and  $MPI_R$  at the lateral wall showed the greatest improvement. Moreover,  $CO_R$  and  $EA_R$  improved significantly, whichever wall was paced. However, at IVS the improvement was greater in patients paced at a concordant site (Table 3). Such a result could explain the improvement in the same global indexes.

**Regional myocardial velocities.** The lack of any significant variation in the regional velocities indicates that BIV had no significant effect on regional myocardial contractility. However, PW velocity is dependent on more than one factor, the assessment of intramyocardial velocity gradient being the most advanced method of detecting regional myocardial velocities.

**Implications.** As TDI is a suitable noninvasive technique for the analysis of regional LV delay, in our opinion it should be implemented in implantation to evaluate in real time the effectiveness of BIV sites. Moreover, since the implantation technique is now advancing toward more

selective sites of pacing, we support the hypothesis that TDI could be useful in tailoring BIV to each individual patient.

**Study limitations.** The first methodological limitation could be the identification of the site of greatest delay on the basis of the  $CO_R$  lengthening alone. It could, indeed, be inferred that the endocardial mapping should have been chosen to identify the most delayed region. However, 1) the latter is invasive; 2) it adds further risk to implantation; 3) ethical considerations preclude a correlation study between TDI and endocardial mapping. Moreover, it could be argued that the final aim of our research is not only to detect the most delayed wall but also to be able to pace it. Since pacing the site of delay can be difficult due to the complexity of the procedure, this research could be of scant clinical relevance. However, such relevance resides in the detection of high percentage discordance between pacing site and delayed site, even though the rationale of BIV is to pace the most delayed site. The problem of how to pace such a site will hopefully be solved by improvement in surgical equipment and techniques.

**Conclusions.** Regional TDI quantitative analysis is an effective noninvasive technique that can assess the severity of the regional delay in activation at each LV wall in LBBB and HF patients who are candidates for BIV treatment. Even if LV performance improved significantly in all patients after BIV, the greatest improvement was found in patients paced at the most delayed site.

#### Acknowledgment

The authors thank Mrs. Mary Monique Rendall, BA (Hons), for reviewing the manuscript.

---

**Reprint requests and correspondence:** Dr. Gerardo Ansalone, via Sesto Rufo 23, 00136 Rome, Italy. E-mail: gansalone@iol.it.

---

#### REFERENCES

1. Cazeau S, Leclercq C, Lavergne T, et al. Effects of multisite biventricular pacing in patients with heart failure and intraventricular conduction delay: for the Multisite Stimulation in Cardiomyopathies (MUSTIC) study investigators. *N Engl J Med* 2001;344:873–80.
2. Auricchio A, Stellbrink C, Block M, et al. Effect of pacing chamber and atrioventricular delay on acute systolic function of paced patients with congestive heart failure. *Circulation* 1999;99:2993–3001.
3. Prinzen FW, Wiman BT, Hunter WC, Faris OP, McVeigh ER. Effects of single and biventricular pacing on the temporal and spatial dynamics of ventricular contraction (abstr). *Circulation* 2000;102:161.
4. Blanc JJ, Etienne Y, Gilard M, et al. Evaluation of different ventricular pacing sites in patients with severe heart failure: results of an acute hemodynamic study. *Circulation* 1997;96:3273–7.
5. Ricci R, Ansalone G, Toscano S, et al, on behalf of the InSync Italian Registry Investigators. Cardiac resynchronization: materials, technique and results. The InSync Italian registry. *Eur Heart J Supplements* 2000;2 Suppl J:J6–15.
6. Garcia-Fernandez MA, Azevedo J, Moreno M, et al. Regional diastolic function in ischaemic heart disease using pulsed wave Doppler tissue imaging. *Eur Heart J* 1999;20:496–505.
7. Hatle L, Sutherland GR. The Gruntzig lecture: regional myocardial function—a new approach. *Eur Heart J* 2000;21:1337–57.

8. Sohn DW, Chai IH, Lee DJ, et al. Assessment of mitral annulus velocity by Doppler Tissue Imaging in the evaluation of left ventricular diastolic function. *J Am Coll Cardiol* 1997;30:474-80.
9. Shan K, Bick RJ, Poindexter BJ, et al. Relation of tissue Doppler derived myocardial velocities to myocardial structure and beta-adrenergic receptor density in humans. *J Am Coll Cardiol* 2000;36:891-6.
10. Schiller NB, Shah PM, Crawford M, et al. Recommendations for quantification of the left ventricle by two-dimensional echocardiography. *J Am Soc Echocardiogr* 1989;2:358-67.
11. Daubert JC, Ritter P, Le Breton H, et al. Permanent left ventricular pacing with transvenous leads inserted into the coronary veins. *Pacing Clin Electrophysiol* 1998;21:239-45.
12. Ansalone G, Giannantoni P, Ricci R, Trambaiolo P, Fedele F, Santini M. Doppler myocardial imaging in patients with heart failure receiving biventricular pacing treatment. *Am Heart J* 2001;142:881-96.
13. Henein MY, Gibson DG. Long axis function in disease. *Heart* 1999;81:229-31.
14. Kerwin WF, Botvinick EH, O'Connell JW, et al. Ventricular contraction abnormalities in dilated cardiomyopathy: effect of biventricular pacing to correct interventricular dyssynchrony. *J Am Coll Cardiol* 2000;35:1221-7.
15. Tsujita-Kuroda Y, Zhang G, Sumita Y, et al. Validity and reproducibility of echocardiographic measurement of left ventricular ejection fraction by acoustic quantification with tissue harmonic imaging technique. *J Am Soc Echocardiogr* 2000;13:300-5.